CONF-960115--1

# Application of Wavelet Theory to Power Distribution Systems for Fault Detection

James Momoh
Department of Electrical Engineering
Howard University
Washington, DC. 20059

D. Tom Rizy
IEEE Senior Member
Oak Ridge National Laboratory
Oak Ridge, Tennesee

## ABSTRACT

In this paper an investigation of the wavelet transform as a means of creating a feature extractor for Artificial Neural Network (ANN) training is presented. The study includes a teresstrial-based 3 phase delta-delta power distribution system. Faults were injected into the system and data was obtained from experimentation. Graphical representations of the feature extractors obtained in the time domain, the frequency domain and the wavelet domain are presented to ascertain the superiority of the wavelet transform feature extractor.

## Introduction

The detection of line faults in a power distribution system continues to pose problems for electric power utilities. In particular, little success has been achieved in detecting the arcing-type high impedance fault which is an obscure, but frequently prevailing type of fault that occurs when energized conductors come in accidental, erratic contact with each other or the ground.

Over the years, researchers have applied many methods to the problem of arcing fault detection. Given a particular detection criteria, the conventional methods are based on setting up computational steps centered around that specific criteria. The criteria used over the years were based on the following characteristics: energy content of the signal, high frequency information compiled over time and statistical information from the current and voltage waveforms[1].

In past years, several attempts have been made to develop a neural network that solves the problem of detecting high impedance faults that go undetected by protective devices. Ebron, and et al. have developed a neural-network approach based on a computer simulation of high impedance faults on a distribution feeder[2]. An additional method computes statistics from the phase currents and uses that as input to a clustering-based neural network for performing fault diagnosis[3].

ANN schemes have been implemented successively for fault diagnosis by many researchers. Three types of neural networks that have proven successful in this area include the back propagation, counter propagation and the clustering-based neural network [4].

To further improve on the accuracy of the ANN require that a suitable feature extractor with capability to distinguish characteristic features such as frequency response of fault, be employed for the task of providing the best patterns to the ANN for training and consultation. In addition to the time domain feature extractor, other candidates include the Fast Fourier Transform, and the Wavelet Transform.

Fourier developed several mathematical tools and published these findings in 1882 in "Analytical Theory of Heat" which described the propagation of heats in solids[5]. One of these tools, the Fourier Transform is used to easily analyze the frequency components of phenomena in the time domain.

Wavelet transforms are based on a set of signals derived from a basic mother wavelet by adjusting the time-shifting and time-dilation parameters. In this way, the wavelet transform isolates and magnifies a specific portion of the input time-domain sequence under investigation.

This paper is divided into the following sections: Section II provides the background theory in the area of transforms, with an illustrative example. Section III describes the Faulted Distribution System used to generate data while Section IV is a discussion of results. Conclusions and future work are presented in Section V.

### Section II - Theoretical Background with Illustrative Examples

The two-sided Fourier Transform is represented by Eq. (1), and was widely used to investigate spectral phenomenon of time domain sequences:

$$F(j\omega) = \frac{1}{\sqrt{2\pi}} \int_{-\infty}^{\infty} f(t) e^{-j\omega t} dt \qquad (1)$$

As advances were made in digital computers, research towards an algoirthm that can more quickly perform the Fourier and its inverse transform was brought forth by Cooley and Tuckey in 1965 [6]. Starting with the discete Fourier Transform (DFT) in Eq. (2), the Fast Fourier Transform (FFT) using the decimation in time decomposition algorithm [6] is shown in Eq. (3).

$$F_k = \sum_{n=0}^{N-1} f_n W_N^{nk} \quad for\ k=0,\ldots,N-1 \qquad (2)$$

where $W_N = e^{-j2\pi/N}$.

$$F_k = G_k + W_N^k H_k \quad for\ k = 0,\ldots,\frac{N}{2}-1$$

$$F_{k+N/2} = G_k - W_N^k H_k \quad for\ k = 0,\ldots,\frac{N}{2}-1 \qquad (3)$$

The components $G_k$ and $H_k$ are computed in (4,5), where:

$$G_k = \sum_{n=0}^{(N/2)-1} f_{2n} W_{N/2}^{nk} \qquad (4)$$

is for even-numbered elements of $f_n$, and

$$H_k = \sum_{n=0}^{(N/2)-1} f_{2n+1} W_{N/2}^{nk} \qquad (5)$$

is for the odd-numbered elements of $f_n$. Together, the computational savings of the FFT becomes $Nlog_2N$ compared to $N^2$ for the DFT.

A wavelet is a square-integrable function with a constant energy, which is usually associated with a wideband transient physical signal. The wavelet transform has been found to be very effective in approaching the analyis of sub-band filtering techniques, quadrature mirror filters, and in signal and image processing [7].

The concept of decomposing a complicated phenomenon into many simpler pieces 'building blocks' was initially developed in the 1930's to handle problems that the Fourier transform was not well suited, and is closely associated with Calderón-Zygmund theory. Further extensions of this theory and Haar's work led to the classification of wavelets by Grossman and Morlet[8].

The Gaussian-envelope mother wavelet chosen for our analysis is the standard Morlet wavelet. It is essentially a windowed FFT except that the Gaussian window is adaptive by the time and dilation parameters (a,b) respectively [9]. The Morlet Wavelet Transform which was originally applied towards oil exploration using seismic wave analysis is based on the historical formulations in 1910 of the mathematician Haar who constructed an orthonormal set of bipolar step functions using dilations [10]. Mother wavelets can be expressed mathematically in the following form:

$$G(a,b) = \frac{1}{\sqrt{2\pi a}} e^{-\frac{1}{2}\left[\frac{(t-b)}{a}\right]^2} e^{j5\frac{(t-b)}{a}} \qquad (6)$$

and exhibit the property of constant energy irregardless of the time shift or dilation parameter values.

The continuous wavelet transform of a function f(t) is:

$$W(a,b) = \int_{-\infty}^{\infty} G(a,b) f(t) dt \qquad (7)$$

which yields a three dimensional representation in terms of time shift and dilation. This can be seen in several mother wavelet generating functions as shown in Figures 1 through 4.

A scheme that can be used to determine the appropriate ranges for the time-shift and dilation parameter is the described further. For discrete values of a,b consider a seqeuence f(kt) recorded from $t_0$ to $t_1$. Let $\Delta$ for a non-periodic sequence f(t) be equal to $(t_1 - t_0)$ and let:

$a_{step} = \dfrac{\Delta}{a_{max}}$, where $a_{max}$ is arbitrarily chosen to be one of the values in the set {10,20,30,...}.

Then, $a_m$ becomes

$$\{0, a_{step}, 2a_{step}, \ldots, a_{max}\}.$$

Define $b_{win} = T/2$, where T corresponds to the smallest time between regions where $\dfrac{df(kt)}{dt} = 0$, and $b_{win}$ corresponds to the Nyquist sampling rate of the smallest frequency component in f(kt).

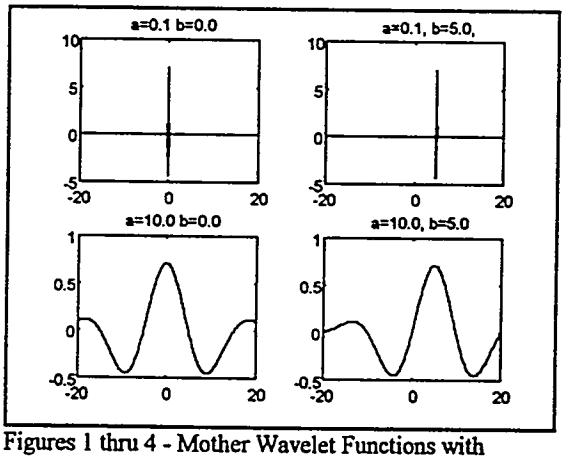


Figures 1 thru 4 - Mother Wavelet Functions with various values of time shift (b) and dilation (a)

Now define $n_{max} = \dfrac{a_{max}}{b_{win}}$ where $1 \le n \le n_{max}$

and $b_n = \{b_{win}, 2b_{win}, \ldots, b_{nmax}\}$.

Therefore, the discrete mother wavelet function can be expressed as:

$$G(a_m, b_n) = \frac{1}{\sqrt{2\pi a_m}} e^{-\frac{1}{2}\left[\frac{(t-b_n)}{a_m}\right]^2} e^{j5\frac{(t-b_n)}{a_m}} \quad (8)$$

Because there are two parameters to be varied, the discrete wavelet transform (DWT) provides data that can be plotted in three-dimensions, where each point on the grid represents the energy of the function when investigated at a specific time ($b_n$), and for a specific dilation or magnification ($a_m$). A flowchart for constructing a DWT for input signal f(t) appears below:

**ALGORITHM FOR BUILDING WAVELET**

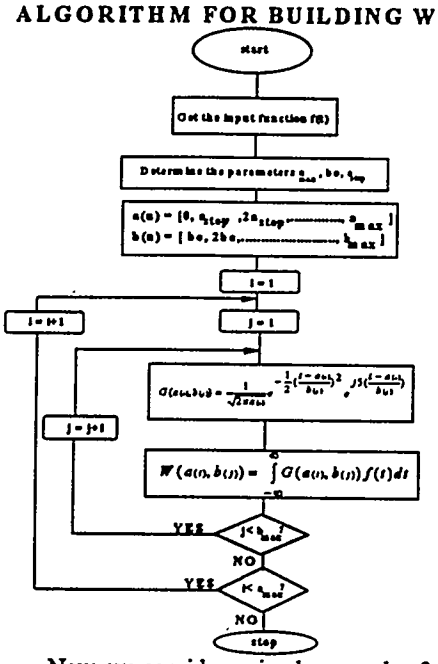


Now, we consider a simple example of a time domain signal with multi-frequency component sine waves represented by Equ. 10 and shown in Figure 5.

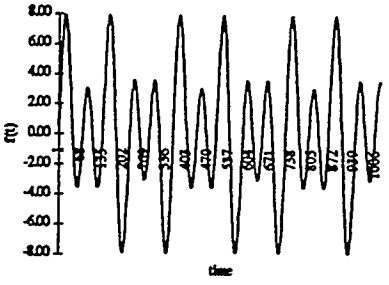


Figure 5 - Input Trajectory of 3 Sinewaves

$$f(kt) = \sin(\frac{kt\pi}{180}) + 3\sin(\frac{3kt\pi}{180}) + 5\sin(\frac{5kt\pi}{180})$$

$$for\ 1 \le kt \le 1024 \quad (10)$$

Figures 6 represents the FFT equivalent of f(kt). Similarily, using the wavelet computer algorithm, we generated 19x20 pixel points and plot the waveform with the various changes in a and b.

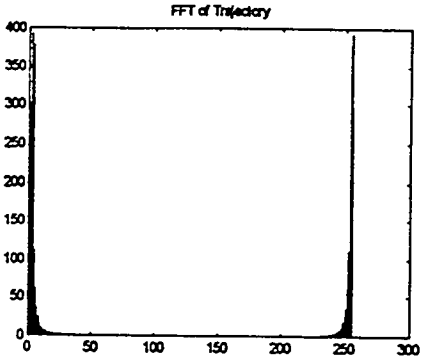


Figure 6- FFT of the Input

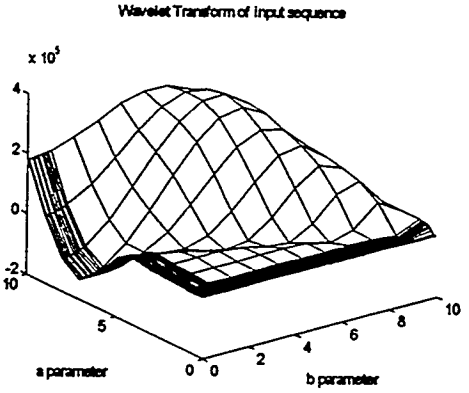


Figure 7 - Wavelet Transform of the Input.
(a and b parameters are respectively the dilation window and time shift)

## Section III - Fault Distribution System Model

The arcing fault system under evaluation is represented by a wye-grounded distribution system at the 4.8kV voltage level which has over 1500 feeder circuits at this voltage level.

For the laboratory generated data, a three phase low-voltage laboratory experiment was staged on an ungrounded test distribution system that represents a part of the model mentionned earlier. Three single phase transformers were connected in a delta-delta or delta-wye configuration to produce a supply of 210:420 volts. The top feeder as shown in Fig 8 represented the faulted feeder, the next one represented a non-faulted feeder with a delta connected load while the last feeder was used as the equivalent of all other non-faulted feeders. For each phase, a single phase 1:1 transformer was connected to a 100W light bulb and a (1/60) hp induction motor. The system was assembled to emulate the multifeeder system that exists at a substation.

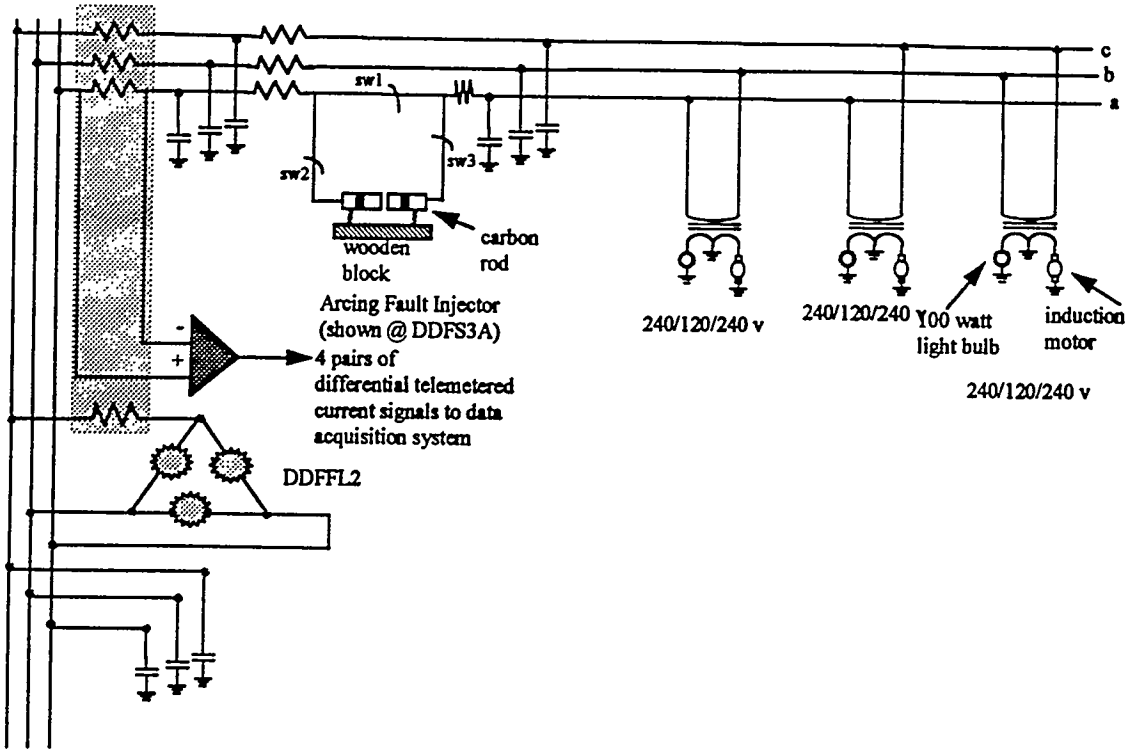


Figure 8: Diagram of the Laboratory Experiment set

Types of faults that may occur in this system include:

line-to-line
single-line-to-ground (SLG)
high-impedance arcing.
three phase
double line to ground (LLG)
double line to line (LL)

Telemetry representing arcing fault conditions was captured using a data acquistion module where each fault was generated by contact of the phase wire to a carbon rod which was mounted on a wooden plank. The position of the carbon rod was changed to represent faults at different locations of the transmission line.

## Section IV - Results

Samples of the telemetry recorded for the ac system under test include DDFS3A and DDFL2 which represent a fault on the source side of the third feeder, and fault on the load side of the second feeder, respectively. The amplitudes of the time domain signal of DDFS3A and DDFL2 were respectively 2.07A and 1.69A. For each case, the current wave of the neutral and of each phase were acquired by a four-channel multifunction data acquisition board. The data was sampled at a sampling rate of 62500 samples/second resulting in 1200 points per case.

WAV3ARC, a feature extraction program implemented in Matlab for Windows was used to produce features in the frequency domain (256 point - FFT) and in the wavelet domain (380 point - DWT) of the time domain data. The time shift and time dilation parameters were varied over the set of values as follows:

a= [.1 .2 .3 .4 .5 .6 .7 .8 .9 1 2 3 4 5 6 7 8 9 10];
b= [0 .1 .2 .3 .4 .5 .6 .7 .8 .9 1 2 3 4 5 6 7 8 9 10];

This means that for each possible (a,b) pair, the DWT corresponding to the energy content of the input signal was computed. Graphically, these points can be displayed as a three-dimensional mesh graph.

Figures 9 through 11 represent the telemetry recorded at channel 2 in the time domain, the FFT of this signal, and the wavelet transform of DDFS3A. Likewise, Figures 12 through 14 represent the same phenomena for DDFL2. From these figures, it is clear that the time domain plots are dominated by a 60 Hz component, and that the FFT shows this domination even further with the harmonic energy content of the same. However, it is difficult to visually discriminate the spectral energy related to the arcs between the two plots in this domain.

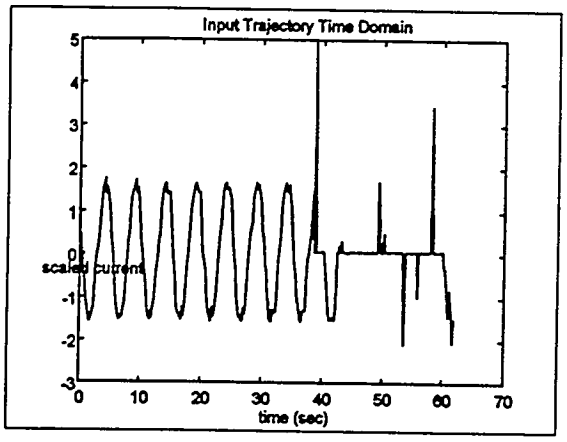


Figure 9- Time domain of DDFS3a (Channel 2)

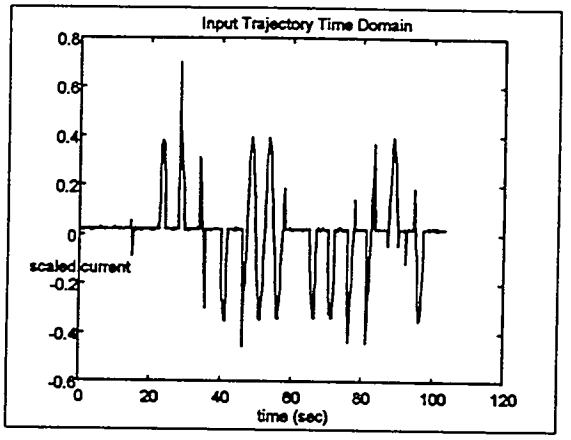


Figure 12- Time domain of DDFL2 (Channel 2)

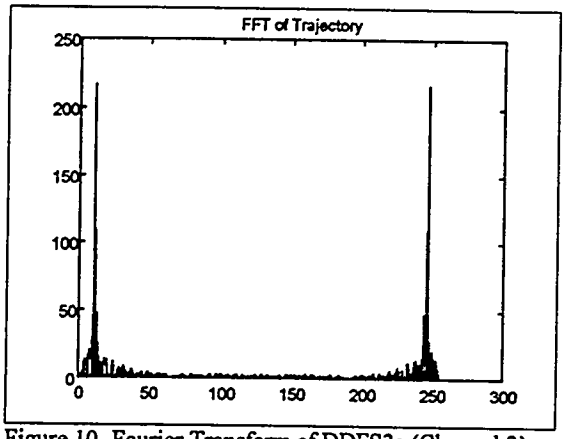


Figure 10- Fourier Transform of DDFS3a (Channel 2)

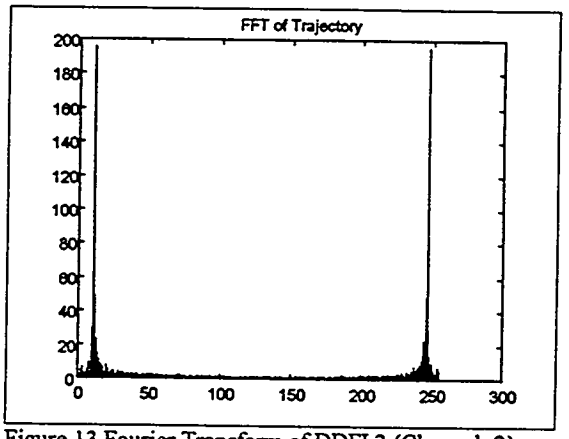


Figure 13 Fourier Transform of DDFL2 (Channel 2)

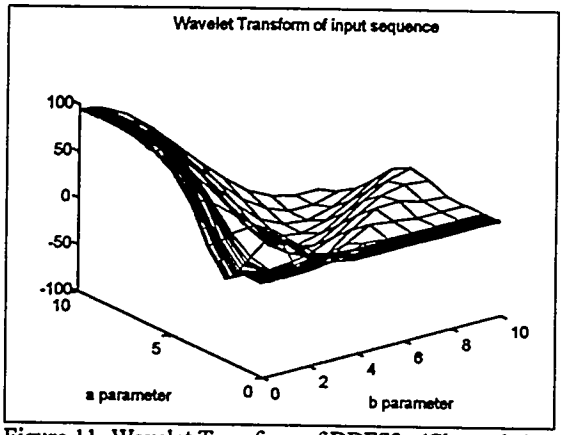


Figure 11- Wavelet Transform of DDFS3a (Channel 2)

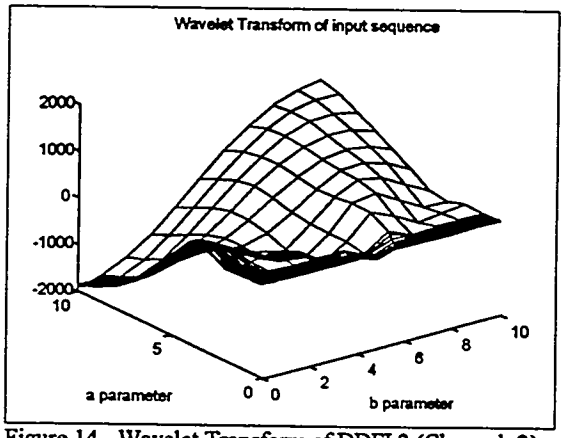


Figure 14- Wavelet Transform of DDFL2 (Channel 2)

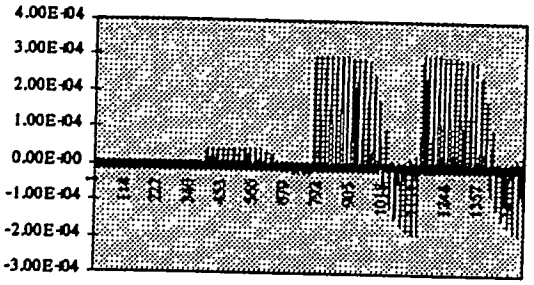


Figure 15 - Wavelet Transform of 4 telemetry channels representing fault DDFL2

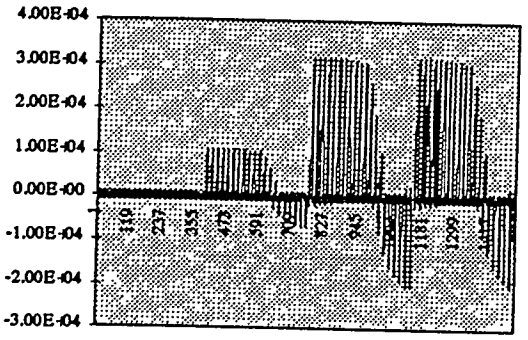


Figure 16 - Wavelet Transform of 4 telemetry channels representing fault DDFS3a

Figures 15 and 16 represent the combined wavelet transform of all 4 channels acquired of the two resepective fault types. These transforms are displayed in two dimensions by holding the dilation parameter "a" constant ,and slicing the 3 dimensional mesh plot along this resulting plane. This is the pattern that will be presented to the ANN. If these two patterns are superimposed, it can be postulated that the ANN will not have a problem in delineating these two patterns.

## Section V - Conclusions

An algorithm for developing a feature extractor suitable for training an Artificial Neural Network for fault diagnosis using the Wavelet Transform has been presented. The feature extractor exhibits a superior set of features (patterns) as compared to feature extractors in the time domain and the frequency domain. Future work includes modifying the ANN Clustering Algorithm to handle larger feature extraction points, and to increase the bus-sizes of our system under test, and to perform comparative analysis of the performance of the wavelet transform feature extractor against the time domain and fast fourier transform feature extractors. From our preliminary findings, it is expected that the existing ANN Clustering Algorithm fault diagnosis tool's accurracy will improve with the implementation of the wavelet transform feature extractor.

## ACKNOWLEDGMENTS

The authors wish to acknowledge the office of Energy Management,US. Department of Energy (DOE) who sponsored in part the research described herein under contract No. DE-AC05-840R 21400. The authors would also like to acknowledge research associates and students (past and present) at Howard University (CESaC) , for their continued support, especially Walter Oliver and Yawo Amegadje who provided computer results.

## REFERENCES

[1] Russel, Don B., and Chinchali, R.P., "A Digital Signal Processing Algorithm for Detecting Arcing Faults on Power Distribution Feeders", *IEEE Trans. on Power Delivery*, Vol. 4, No. 1, Jan 1989, pp.132-140.

[2] Ebron, S., Lubkeman, D., and White, D., "A Neural Network Approach to the Detection of Incipient Faults on Power Distribution Feeders," *IEEE Trans. on Power Delivery*, Vol. 5, No. 2, April 1990, pp. 905-914.

[3] J. Momoh, L. Dias, K. Butler, D. Laird, "Selection of Artificial Neural Networks for Distribution System Fault Diagnosis", *4th Intelligent Systems Applications to Power Systems*, 1994, pp.37-43.

[4] T. Dalstein, D.J. Sobajic, B. Kulicke, Y.H. Pao, "Neural Network Approach to Fault Direction Direction Identification in Electric Power Systems", *Proceedings of the 1993 North American Power Simposium*, pp.290-299.

[5] "Joseph Fourier Looking Back 1768-1830", Université Joseph Fourier: Grenoble I, Internet Hypertext.

[6] S.A. Treeter, 'Introduction to Discrete-Time Signal Processing', *John Wiley & Sons*, 1976, pp.284-85.

[7] "Causal Analytical Wavelet Transform", *Optical Engineering*, Sept. 1992, vol 31 no. 9, pp1825-29.

[8] Bjorn Jawerth and Wim Sweldens, "An Overview of Wavelet Based Multiresolution Analyses", *Original Manuscript developed at the Dept. of Mathematics, Univ. of S. Carolina*

*under DARPA Grant AFOSR F49620-93-1-0083.*, 1995.

[9] A. Grossmann and J. Morlet, " Decomposition of Hardy Functions into Square Integrable Waveletsof Constant Shape," *SIAM J.Math.Anal.*, Vol 15, No.4, pp723-736, July 1984.

[10] A. Haar, Math. ANN. 69,331 (1910)

## DISCLAIMER